J. theor. Biol. (1995) **175,** 27–37

Reflection-Polarization Patterns at Flat Water Surfaces and their Relevance for Insect Polarization Vision

GÁBOR HORVÁTH

Biophysics Group, Department of Atomic Physics, Loránd Eötvös University, H-1088 Budapest, Puskin u. 5–7., Hungary

(*Received on* 30 *November* 1993, *Accepted in revised form on* 19 *October* 1994)

It has recently been shown that horizontally polarized ultraviolet light reflected from the surface of water is the main optical cue for habitat finding by insects living in, on, or near water. What are the polarization properties that make the skylight reflected by water attractive to flying water insects in nature? In this paper, as an approach to this problem, the patterns of the degree and direction of polarization of skylight visible over a flat water surface are computed for unpolarized light from an overcast sky and for partially polarized skylight as a function of the zenith distance of the sun. These patterns are compared with the corresponding celestial polarization patterns. The effect of depolarizing clouds on these reflection-polarization patterns is demonstrated. Reflectivity patterns of a flat water surface are also calculated for clear and overcast skies. The polarization of the blue sky is described by the semi-empirical Rayleigh model. It is assumed that the reflection polarization of skylight at the water surface is governed by the Fresnel formulae. The effect of some modifying factors on the reflection-polarization field is briefly discussed. The adaptations of the visual system of insects living in, on, or near water to reflection-polarization patterns at water surfaces are briefly reviewed and discussed by means of three representative species: the waterstrider (*Gerris lacustris*), the backswimmer (*Notonecta glauca*), and the dragonfly (*Hemicordulia tau*).

1. Introduction

Polarization of light is a common optical phenomenon (Können, 1985). Scattering and reflection are the most important ways in which polarized light originates in nature. Consequently, one of the main sources of partially linearly polarized light is the blue sky owing to the scattering of sunlight within the Earth's atmosphere (Coulson, 1988). The underwater world is also strongly polarized because of light scattering in water (Jerlov, 1976). The third main source is the light polarized by reflection from shiny surfaces, e.g. water surfaces or moist substrates (Können, 1985). In practice, the human eye is virtually polarization-blind, therefore the polarization vision of animals became a topic of research only after von Frisch (1949) discovered that bees are able to navigate by celestial polarization patterns. Since then some important properties of the underlying mechanism have been elucidated (Waterman, 1981; Rossel, 1989; Wehner, 1989). Much less attention has been paid to the physiologic optical role of polarized skylight reflected from the water surface (Schwind, 1991).

Although the polarization of water-surface-reflected skylight is a striking optical phenomenon in the natural environment and its characteristics are more or less qualitatively known, reflection-polarization patterns (RPPs) have nevertheless never been quantitatively investigated in detail previously. On the one hand, it is difficult to measure (e.g. by means of remote sensing) these patterns over natural water surfaces, so most of the measurements are made in the laboratory (e.g. Chen & Rao, 1968). On the other hand, it is impossible to compute these patterns at optically rough, undulating water surfaces—theoretical calculations must be restricted to describing the reflection polarization of skylight at the flat air–water interface.

Recently many water insects and insects living on moist substrates have proved to be sensitive to

polarized light (Schwind, 1991; Bartsch, 1991). Their polarization vision is associated predominantly with the RPP (Schwind & Horváth, 1993). Water insects can easily be trapped by artificial reflecting surfaces (Schwind, 1991), which implies that the reflection of skylight from water surfaces is an important factor in their habitat finding. Some properties that make the skylight reflected by artificial surfaces (with different spectral, polarization and reflectivity characteristics) attractive to flying water insects were elucidated by Schwind (1985*a*, 1991). Is the attractiveness of a water surface in nature also affected by the gradient of the RPP? As an approach to this problem, the patterns of the degree and direction of polarization of skylight visible over a flat water surface are computed for unpolarized light from an overcast sky and for partially polarized skylight as a function of the zenith distance of the sun. They are compared with the corresponding celestial polarization patterns. The effect of depolarizing clouds on the RPPs is demonstrated. Reflectivity patterns of a flat water surface are also calculated for clear and overcast skies. Surface waves, particles in water, reflection from the bottom of water and refraction polarization at the water surface more or less modify the RPPs. The effect of these factors on the RPP is briefly discussed. This is the first attempt to calculate RPPs at flat water surfaces in detail. A preliminary account of these patterns has appeared recently (Schwind & Horváth, 1993). In the Discussion, I briefly review the known adaptations of the visual system of insects living in, on, or, near water to polarized skylight reflected from the water surface, in three representative species: the waterstrider (*Gerris lacustris*), the backswimmer (*Notonecta glauca*), and the dragonfly (*Hemicordulia tau*).

2. Methods

The three-dimensional celestial hemisphere was represented in two dimensions by a polar coordinate system, where the angular distance θ from the zenith and φ from the solar meridian are measured radially and tangentially, respectively. In this two-dimensional coordinate system the zenith is at the origin and the horizon corresponds to the outermost circle. To display the RPP of skylight visible over a flat water surface, a two-dimensional polar coordinate system positioned parallel to the air–water interface was used. This system of coordinates is called the ''mirror-system''. In the mirror-system, the ''mirror zenith'' (nadir), ''mirror sun'', ''mirror solar meridian'' and ''mirror anti-solar meridian'' correspond to the zenith, sun, solar and anti-solar meridian of the celestial system, respectively. In the calculations it was assumed that (i) the air–water interface is flat, without ripples and (ii) the polarization of light arising from reflection on the bottom of the water and/or from scattering by particles suspended in water is negligible in comparison with the reflection polarization at the water surface.

The degree and direction of polarization of skylight are given in Appendices A and B. Using the Fresnel formulae, the reflection-polarization features of the air–water interface derived for unpolarized and partially linearly polarized incident skylight are given in Appendices C and D. The polarization of the sky was described by the semi-empirical Rayleigh model, which can be considered as a relatively good approximation (Coulson, 1988). The regions of the sky and the flat water surface, with different degrees and directions of polarization values and reflectivities, are grey-scale shaded in the illustrations. Fractal-like patterns of clouds were generated by the common algorithm of Brownian motion (Mandelbrot, 1983). The light radiated by clouds was assumed to be unpolarized.

3. Results

3.1. REFLECTION–POLARIZATION PATTERNS

The RPPs of skylight were investigated for three different meteorological conditions: (i) clear sky, (ii) partially cloudy sky and (iii) overcast sky. The simplest polarization distribution on the water surface occurs under overcast skies (Figs 3F, 4F, 7E). In this case, the polarization maximum of reflected light is located in a band—referred to as the Brewster zone in this work—centered at a nadir angle of 53° at all azimuths around the point of observation. The reflection-polarization field is everywhere symmetric in azimuth. For a clear atmosphere, the polarization and nonisotropic nature of skylight modify the picture. Figure 1 shows the celestial distribution of the degree of polarization of skylight for different zenith distances of the sun.

The sky is usually partially cloudy, making some parts of the celestial polarization pattern (Figs 1 and 5) hidden. Desert ants and honeybees, for instance, orientate on the basis of patches of the celestial polarization pattern when the sun is occluded by clouds (Fent, 1986; Wehner, 1989). Figure 2 demonstrates this situation. Here, the patterns of the degree of polarization (Fig. 1) are partly covered by clouds radiating unpolarized light. Figure 3A–D shows the pattern of the degree of polarization of reflected skylight visible over a flat water surface under clear skies for different zenith distances of the sun.

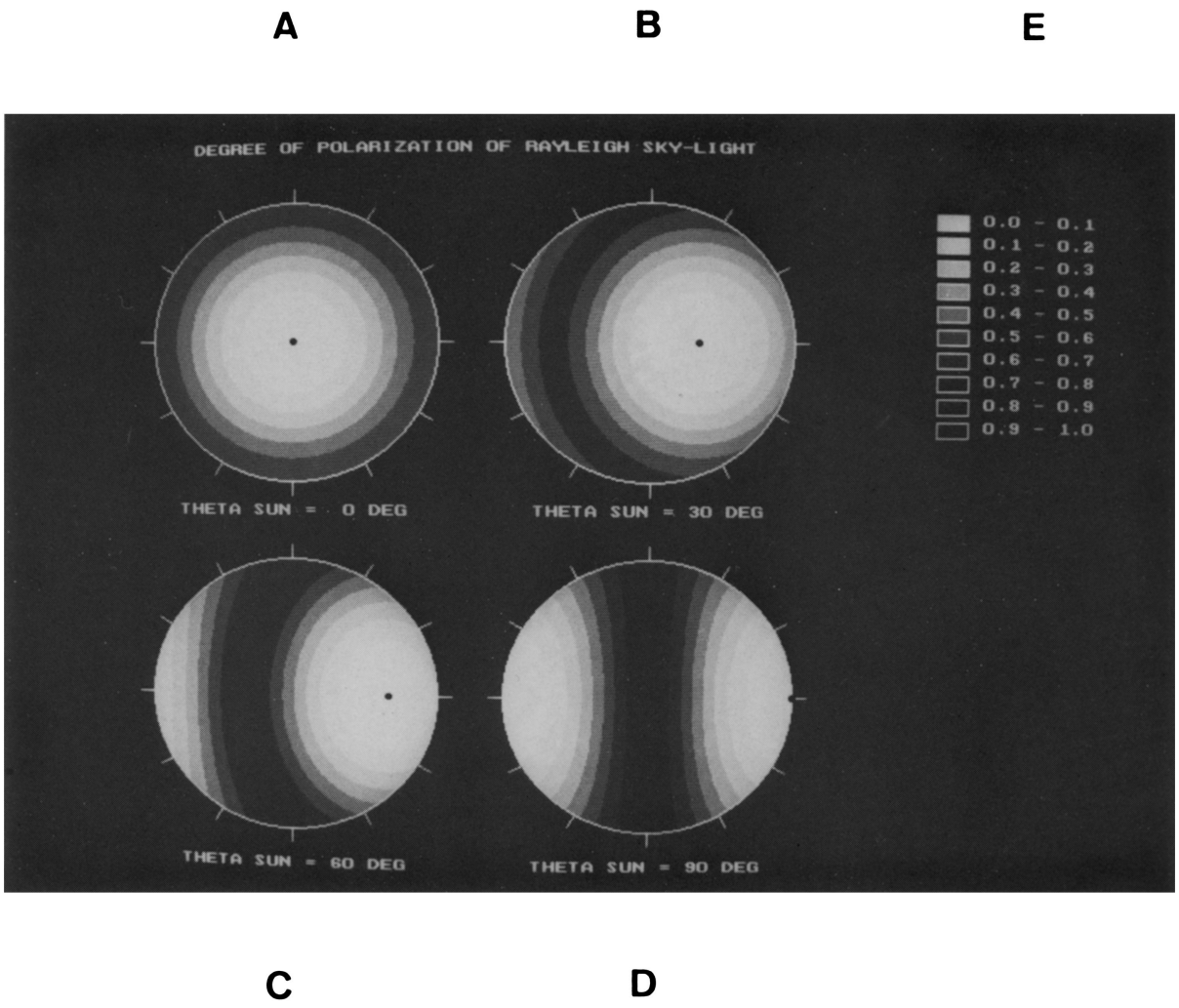

FIG. 1. Two-dimensional pattern of the degree of polarization of skylight under clear skies for different zenith distances θ_s of the sun. (A) $\theta_s = 0^\circ$ (sun at the zenith), (B) $\theta_s = 30^\circ$, (C) $\theta_s = 60^\circ$, (D) $\theta_s = 90^\circ$ (sun at the horizon). The sun is indicated by a dot. (E) Shades corresponding to the different intervals of the degree of polarization ranging from 0 to 1 in steps of 0.1. Here and in the following figures the celestial hemisphere and its mirror image visible at the flat water surface are represented in a two-dimensional coordinate system. The zenith and the nadir are at the origin and the horizon is represented by the outermost circle. The angular distances θ and φ from the zenith and from the solar meridian are measured radially and tangentially, respectively.

(facing p. 28)

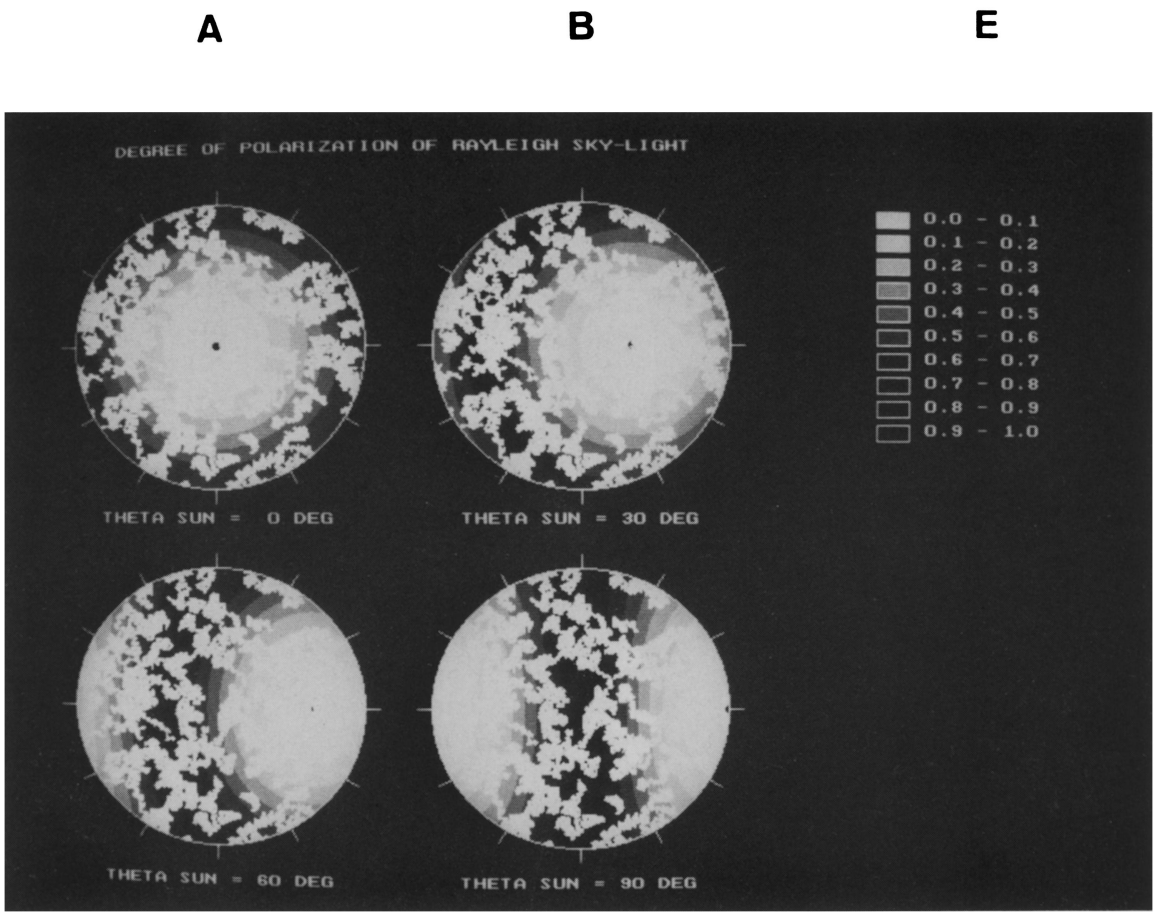

FIG. 2. As Fig. 1 with clouds, which are white, as it was assumed that the light radiated by them is unpolarized.

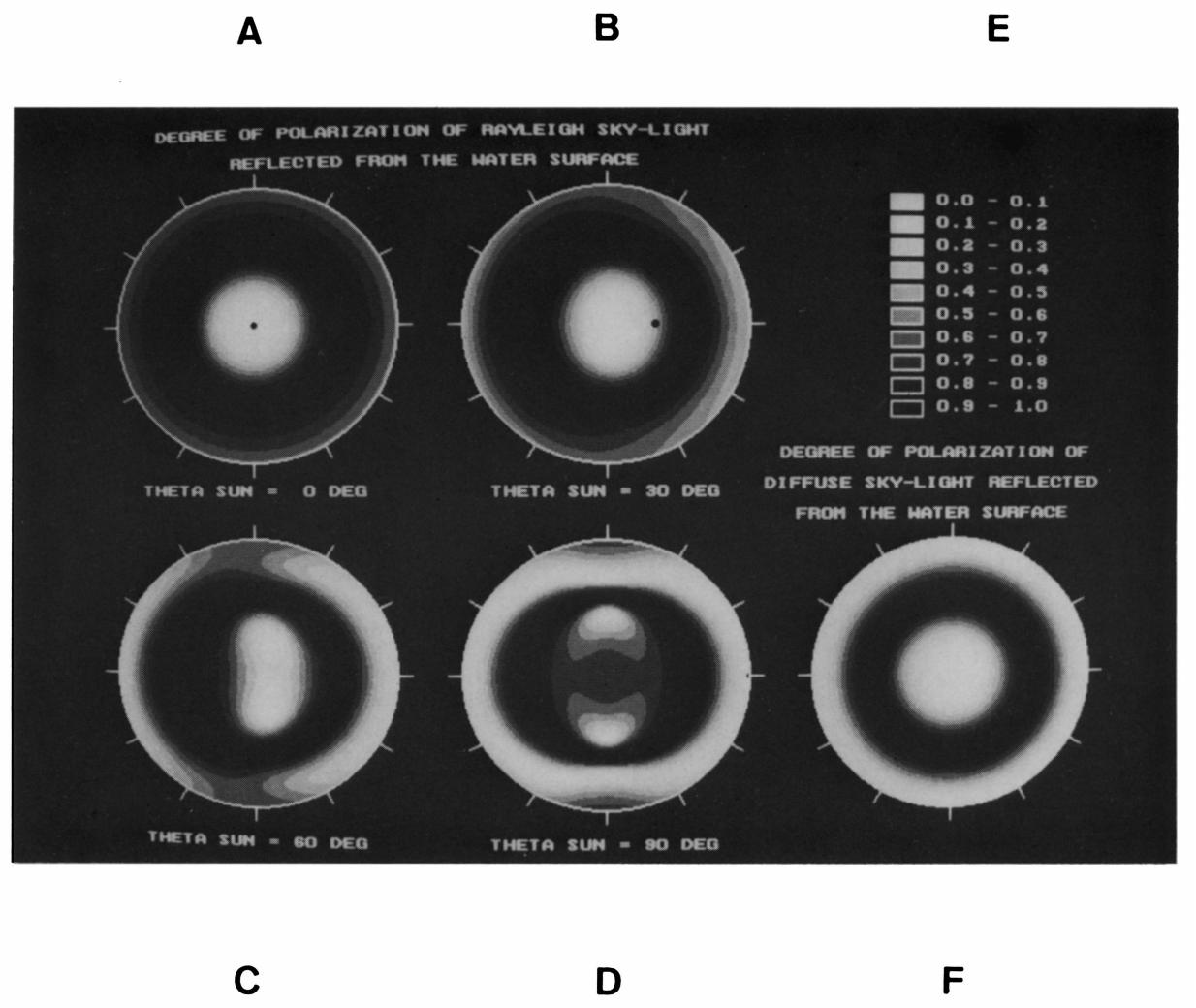

FIG. 3. Pattern of the degree of polarization of skylight reflected from a flat water surface under clear skies for different zenith distances θ_s of the sun. (A) $\theta_s = 0^\circ$, (B) $\theta_s = 30^\circ$, (C) $\theta_s = 60^\circ$, (D) $\theta_s = 90^\circ$. The mirror sun is indicated by a dot. (E) Shades corresponding to the different intervals of the degree of polarization of reflected light ranging from 0 to 1 in steps of 0.1. (F) As for panels (A–D) for unpolarized light from an overcast sky.

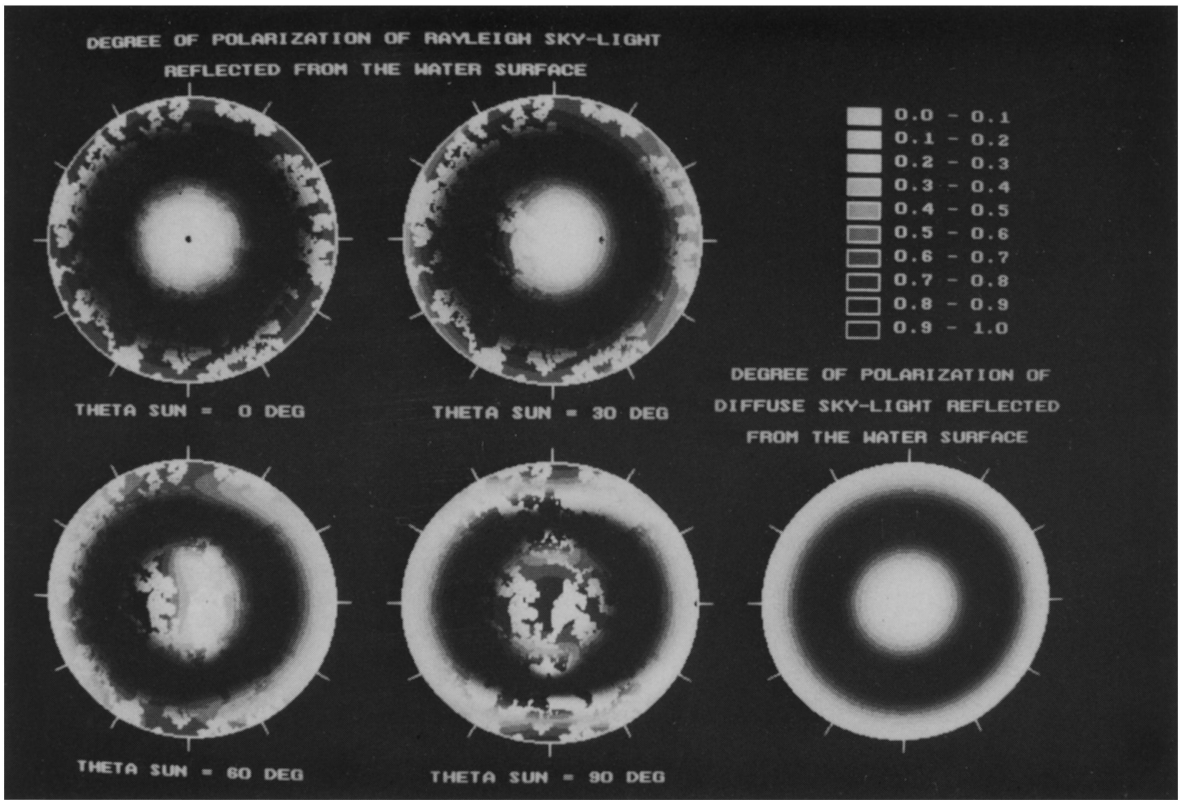

FIG. 4. As Fig. 3 with the same clouds as those in Fig. 2. The mirror clouds, visible at the flat water surface, are heterogeneously shaded because the reflected cloud light is partially linearly polarized, the degree of polarization of which depends on the direction of view.

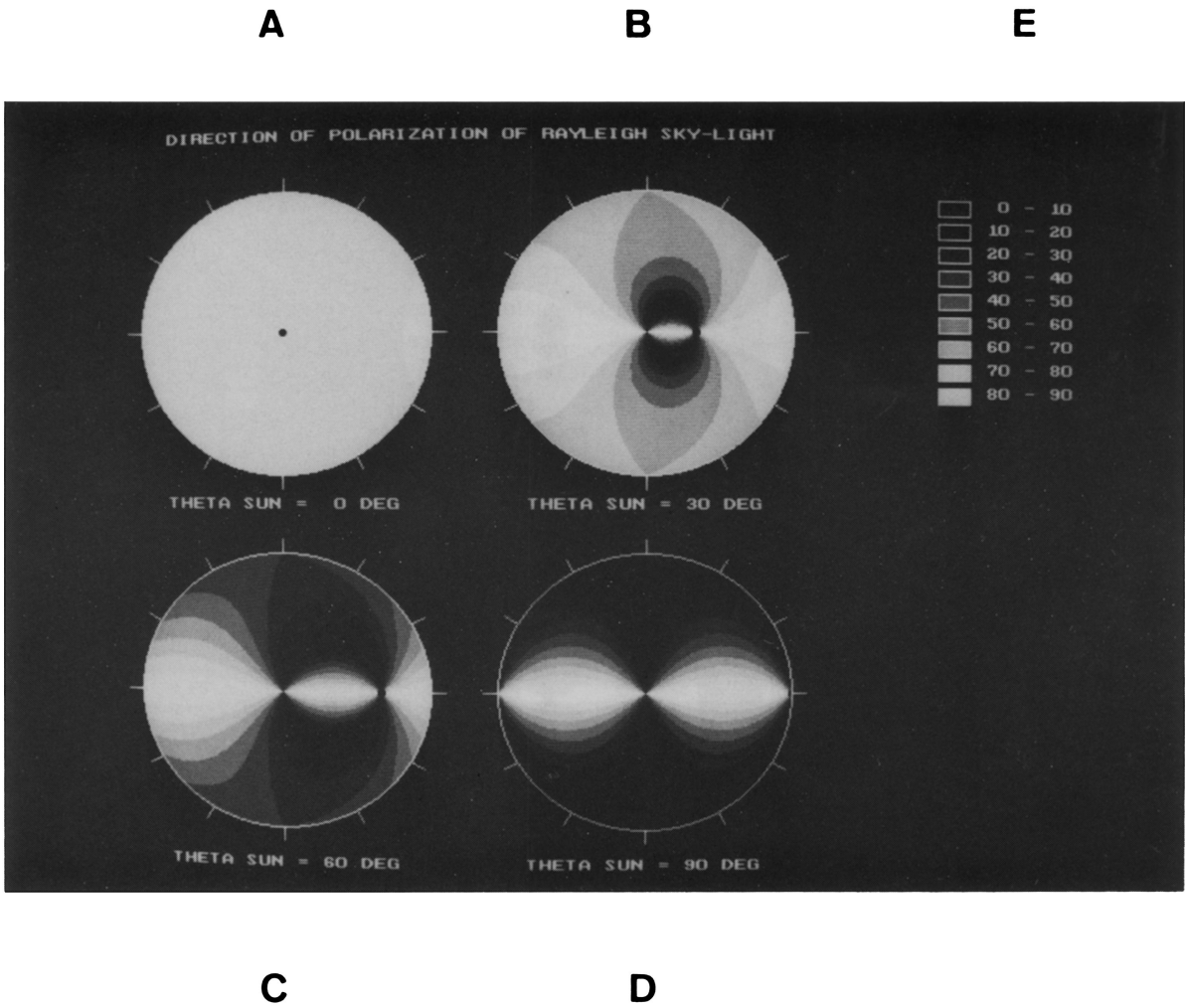

FIG. 5. As Fig. 1 for the direction of polarization of skylight ranging from 0° to 90° in steps of 10° measured from the meridian of the point observed in the clear sky. Since all E-vectors of the celestial polarization pattern are horizontal when the sun is at the zenith, pattern (A) is homogeneous white.

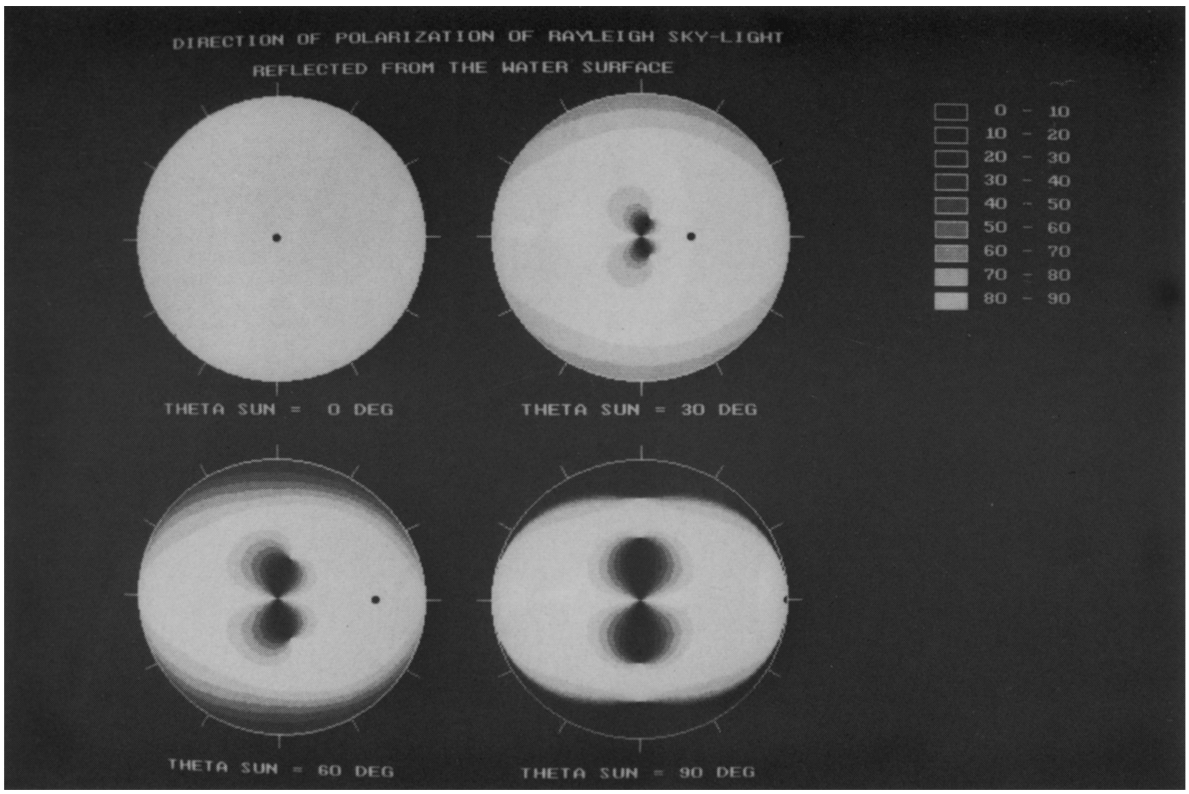

FIG. 6. Pattern of the direction of polarization of skylight reflected from a flat water surface under clear skies for different zenith distances θ_s of the sun. (A) $\theta_s = 0^\circ$, (B) $\theta_s = 30^\circ$, (C) $\theta_s = 60^\circ$, (D) $\theta_s = 90^\circ$. The mirror sun is indicated by a dot. Since all reflected E-vectors are horizontal when the sun is at the zenith pattern (A) is homogeneous white. (E) Shades corresponding to the different intervals of the direction of polarization of reflected skylight ranging from 0° to 90° in steps of 10° measured from the mirror meridian of the point observed at the water surface.

Figure 3F shows the same pattern calculated for unpolarized light from an overcast sky. Figure 4 shows the pattern of the degree of polarization of reflected skylight when the sky is partially covered by clouds. Contrary to the uniformly white colour of the clouds in Fig. 2, the "mirror clouds" in Fig. 4 are heterogeneously shaded because the degree of polarization of reflected light for unpolarized incident light depends on the angle of view as can be seen in Fig. 3F (or 4F).

Comparing the RPP calculated for clear skies (Fig. 3A–D) with that for an overcast sky (Fig. 3F or 4F), one can see that for smaller (Fig. 3A, B) and larger (Fig. 3C, D) zenith distances of the sun the former is considerably different from the latter outside and inside the Brewster zone, respectively. The reflected light of the clouds has the same polarization characteristics as those of an overcast sky (Fig. 3F or 4F). Thus when the sun is near the zenith, outside the Brewster zone, the mirror clouds greatly influence the calculated RPPs for clear skies (Fig. 4A, B). For larger zenith distances of the sun the impact of mirror clouds is considerable inside the Brewster zone (Fig. 4C, D). The Brewster zone itself is hardly influenced by the mirror clouds, because the light reflected from this annular region of the water surface is always strongly horizontally polarized, irrespective of the polarization state of incident light.

The pattern of the direction of polarization of skylight (the celestial E-vector distribution) is shown in Fig. 5 as a function of the zenith distance of the sun. The corresponding pattern of the direction of polarization of skylight reflected from a flat water surface is shown in Fig. 6. (When the sun is at the zenith, all celestial and reflected E-vectors are horizontal). Irrespective of the meteorological conditions and of the zenith distance of the sun, all RPPs have a characteristic annular Brewster zone with a strong horizontal polarization (Figs 3, 4, 6). Under clear skies the shape of this Brewster zone slightly depends on the zenith distance of the sun; it is more extended towards the anti-solar point. When the sun is on the horizon, the Brewster zone is maximally extended towards and away from the sun and becomes narrowest perpendicular to this direction (Figs 3D, 4D, 6D). For small zenith distances of the sun, the reflection polarization of skylight is mainly horizontal (Fig. 6A, B). At larger zenith distances of the sun, the flat water surface is mainly horizontally polarized both in the direction of the sun and opposite to it, but it is mainly vertically polarized near the nadir at right angles to the mirror solar meridian (Fig. 6C, D) just like the blue sky itself (Fig. 5C, D). This vertically polarized region of the water surface extends normally to the solar meridian as the sun approaches the horizon (Fig. 6B, C) and at twilight (sun at the horizon) it reaches the horizon taking there an extended bowed shape (Fig. 6D).

On the water surface under an overcast sky there is a neutral point at the nadir and a narrow annular neutral zone at the horizon (Fig. 3F). Under a clear sky the latter neutral zone disappears and only the neutral point inside the Brewster zone remains when the sun is at the zenith (Fig. 3A). As the sun approaches the horizon this neutral point becomes elongated (Fig. 3B) then splits into two different neutral points (Fig. 3C). As the sun sinks, these neutral points move off each other, and at twilight they are positioned at about 45° from the nadir at right angles to the mirror solar meridian (Fig. 3D). When the sun is at the horizon there are two additional neutral points outside the Brewster zone perpendicularly to the mirror solar meridian, and two further extended bow-shaped neutral regions towards the sun and opposite to it (Fig. 3D). These neutral points and zones are the regions of the water surface where the horizontal polarization of reflected skylight switches to vertical (Fig. 6B–D).

3.2 REFLECTIVITY PATTERNS

Figure 7A–D shows the two-dimensional pattern of reflectivity of a flat air-water interface calculated for different zenith distances of the sun. Figure 7E shows the reflectivity pattern of a flat water surface for diffuse unpolarized light from an overcast sky. Comparing Fig. 7A–D with 7E, one can establish that they all have a quasi-cylindrical symmetry for reflectivity values larger than 7%, i.e. for directions of observation larger than 65° from the vertical. One can see in Fig. 7 that as the sun approaches the horizon, the contour lines of equal reflectivity gradually become elongated perpendicularly to the solar meridian. The two patches in Fig. 7C, D show those regions of the water surface where the reflectivity is less than 2%. Thus two dark patches can be seen on the water surface at 90° from the sun when it is near the horizon. The surface is clearly more transparent at these patches.

The occurrence of these patches and the elongation of the reflectivity contour lines at 90° from the solar meridian, for the sun near the horizon, are explained in the following way. The reflectivity is very small if (i) the degree of vertically polarized incident light is large, and (ii) the incident angle is near to or smaller than the Brewster angle. This is because the value of the amplitude reflection coefficient ρ_v [see eqn (C.3) in Appendix C] is very small for incident angles near to or smaller than the Brewster angle. As the sun approaches the horizon the band of the maximum

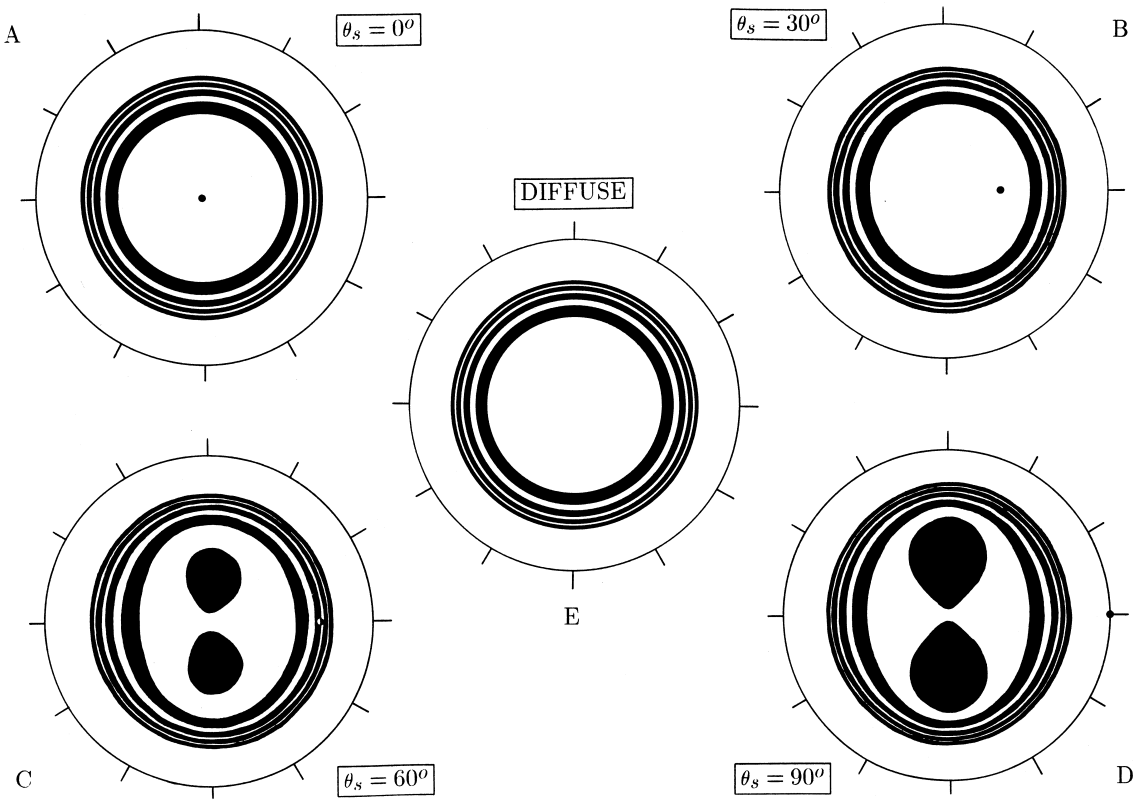

FIG. 7. Contour lines of equal reflectivity of a flat water surface under clear skies for different zenith distances θ_s of the sun (A–D) and for unpolarized light from an overcast sky (E). The position of the sun is indicated by a dot. In patterns (C) and (D), the two black patches represent the regions of the water surface where the reflectivity is less than 2%. In all patterns the contour lines belong to reflectivity values of 3, 4, . . ., 9, 10% from the centre towards the periphery; the outermost circle (illustrating the horizon) represents a reflectivity value of 100%. For clarity every second reflectivity region is black.

degree of polarization of the sky nears the zenith (Fig. 1). The skylight from this zone satisfies condition (i). Furthermore condition (ii) is also fulfilled in the patches of the water surface shown in Fig. 7C, D. Conditions (i) and (ii) are satisfied in a larger angular interval (measured from the zenith) at 90° from the solar meridian than parallel to it. This results in the elongation of the reflectivity contour lines perpendicularly to the direction of the sun when it is near the horizon (Fig. 7C, D). For smaller zenith distances of the sun at least one of the above two conditions is not satisfied at any point on the water surface, so the patches of very low reflectivity disappear (Fig. 7A, B).

The RPPs visible over flat water surfaces under clear skies have gradients of reflectivity (Fig. 7), degrees (Fig. 3) and directions (Fig. 6) of polarization that are quite strong at larger zenith distances of the sun, i.e. at twilight (Figs 3C, D, 6C, D and 7C, D). Under an overcast sky, these water-surface-specific gradients of the degree of polarization and reflectivity can also be observed (Figs 3F, 4F and 7E), but now there is no gradient in the direction of polarization (because the reflected E-vector is always horizontal). These different gradients are often associated with the same regions of the water surface: where the reflectivity gradient is large, so too are the gradients for the degree and direction of polarization. This can be seen, for example, in the case of the characteristic butterfly-like pattern inside the Brewster zone in Fig. 6C, D. This butterfly-like pattern coincides with the two neutral points of the pattern of degree of polarization (Fig. 3C, D) and with the dark patches of the reflectivity pattern (Fig. 7C, D).

4. Discussion

Since most of the light around us is reflected from different objects, reflection polarization predominates; this is linear, and at rough surfaces (e.g. grass plains or a mass of leaves) it is tangentially directed with respect to the sun by clear skies (Können, 1985). The flat surface of still water creates reflections with mainly horizontal polarization. Then the source of light is not always the sun, but could be a section of the sky. The water surface reflects UV light (down to a wavelength

of 310 nm) better than visible light, but plants reflect less UV than green light (Gates, 1980; Coulson, 1988). In the UV range of the spectrum, therefore, water surfaces are more distinct from their surroundings than in the visible range. Hence, in nature the RPP of a water surface consists of horizontally-polarized UV-biased light, and often displays strong gradients (Figs 3, 4, 6 and 7). These RPPs are inserted into a predominantly tangentially polarized (with respect to the sun) and less UV-reflective world. This suggests that the RPP of a flat water surfaces could be a prominent optical cue for animals whose visual system can discriminate the plane of polarization (Schwind, 1985*a*, 1991; Schwind & Horváth, 1993).

Here, we are dealing with the repolarization of skylight reflected from the air–water interface in order to infer the physiologic optical role of the RPP in polarization vision, orientation and habitat finding by water insects. Until now, this topic has not been included in the sphere of interest of biologists dealing with polarization vision of animals. For a long time it has been considered unlikely that animals could orient to the polarization of light reflected from water surfaces (Stockhammer, 1959; Waterman, 1981). It was thought that the RPP may vary too much in space and time because of the water ripples. Nevertheless, work by Schwind (1985*a*, *b*, 1991) highlighted the biological relevance of this pattern.

Many insects and other arthropods are able to detect the plane of vibration of linearly polarized light (Waterman, 1981; Rossel, 1989). In most of these animals their polarization vision is associated with their orientation by means of the celestial polarization pattern (Laughlin, 1976; Labhart, 1980, 1986; Horridge *et al*., 1983; Hardie, 1984; Labhart *et al*., 1984). Usually, the polarization-sensitive receptors are gathered into a specialized eye region (Wehner & Strasser, 1985) which I shall call the polarization-sensitive area (PSA). Such a PSA exists in honeybees, desert ants, flies and crickets on the dorsal marginal eye region (Rossel, 1989), which is an adaptation of their visual system to the celestial polarization pattern. Insects living in, on, or near water possess a ventral polarization-sensitive eye region which detects the RPP of skylight (Schwind, 1991; Schwind & Horváth, 1993). This ventral PSA could be involved in horizon detection by dragonflies (Laughlin, 1976; Laughlin & McGinnes, 1978); in detecting objects under or on the water surface by waterstriders (Varjú & Horváth, 1989); and in detection and identification of water by all water insects (Schwind, 1991).

Schwind (1991) has shown that some aquatic insects do not find their habitats phototactically, and it is not the dark appearance of some ponds that attracts them. Neither is glitter from waves necessary, and the surface-reflected image is not decisive for the attractiveness of water either. Schwind found that horizontally polarized light is a prerequisite for the following insects to recognize their habitats: bugs and beetles living as adults in, on, or near water; beetles living in moist decaying plant debris or dung; nematocerans, living as adults on land, but developing in water. Some insects, however, may make use of other cues to detect water bodies: insects inhabiting running waters do not locate their habitats by means of polarization vision at all because polarization is distorted by waves (Zwick, 1990). Aquatic insects and those living in moist substrates are also influenced in their choice of habitats by non-optical factors (Westphal, 1984), but their visual system is the first that becomes operative as a long-distance water detector.

The minimum requirement for water detection by a compound eye is a blue or UV-sensitive ventral subsystem with horizontal microvilli (e.g. ventral eyes in whirligig beetles: Klaus Vogt, personal communication). Nevertheless an orthogonal polarization analyser functioning in the UV range, is more suitable (e.g. the ventral PSA in backswimmers; Schwind, 1985*a*). Such a system can identify water, with the exception of those regions of the water surface where the reflected skylight is mainly vertically polarized (Fig. 6C, D) or almost neutral (Figs 3 and 4) or has very small reflectivity (Fig. 7C, D). It is advantageous if the water detector functions in the blue or UV range of the spectrum, because the environment and the bottoms of water bodies tend to reflect much less in these spectral ranges (Gates, 1980; Können, 1985). Under clear skies, the degree and direction of polarization gradients of the water surface and the structure of a rough water surface with ripples and water plants may also be involved in detecting and identifying water. From the brief review below we can see that the polarization vision of water insects is also adapted to the RPP, just as the dorsal PSA of the above-mentioned insects is adapted to the celestial polarization pattern.

4.1. FACTORS MODIFYING THE RPP

The reflection-polarization characteristics of natural water surfaces depend not only on illumination but also to a considerable extent upon the presence or absence of waves or ripples. In smaller bodies of water—for example puddles, ponds, ditches preferred and inhabited by water insects—surface ripples disappear quickly (Jelley, 1989). Under an overcast sky the light reflected by an undulating water surface has mainly horizontal and relatively strong polarization (Können, 1985). Under clear skies, the polarization of

an undulating water surface is tangentially directed with respect to the sun and the degree of polarization is usually less than in reflection by flat water surfaces (Können, 1985). At twilight, an undulating water surface is horizontally polarized both in the direction of the sun and opposite to it, but it is vertically polarized at 90° from the sun. At about 40° from the sun, the horizontal polarization switches to vertical so that the reflected light is unpolarized (neutral point) (Können, 1985). Since insects living in (e.g. backswimmers and whirligig beetles) or on (e.g. waterstriders) water find their food mainly on the water surface by means of prey-generated ripples (e.g. Murphey, 1971; Wiese, 1972), and their intraspecific communication is based also on water ripples (e.g. Wilcox, 1972; Bendele, 1986), it is important for them that the water surface remains as still as possible. Therefore, water insects prefer predominantly standing or slowly flowing small water bodies with a flat surface. The polarization characteristics of these habitats can be well described by the RPPs presented in this work.

A further modifying factor is polarization which arises from the scattering of underwater light, a major factor for aquatic animals living in the seas and oceans (e.g. Waterman, 1981; Hawryshyn, 1992). This effect is dominant in greater bodies of water, rather than in the small, still water bodies (e.g. ponds, ditches, puddles or pools) inhabited by water insects, except when the latter habitats are very turbid with a strong underwater polarization due to a dense growth of phytoplankton.

A more important modifying factor is the effect of light reflected from the bottom of small water bodies. This bottom-reflected light is generally unpolarized due to the diffuse reflection, but it becomes mainly vertically polarized after transmission through the water surface because of refraction. Consequently, the bottom-reflected partially vertically polarized light can depolarize to some extent the surface-reflected mainly horizontally polarized light. This is of great biological importance because the polarization-sensitive visual system of water insects must function in that range of the spectrum in which the reflection of the bottom is negligible in comparison with the surface reflection (Schwind, 1991). The ultraviolet range is ideal in this respect (Gates, 1980; Coulson, 1988).

4.2. POLARIZATION VISION IN THE VENTRAL EYE REGION OF THE WATERSTRIDER *GERRIS LACUSTRIS*

In the apposition compound eye of the waterstrider *Gerris lacustris* there are two types of ommatidia: dorsal-equatorial and ventral (Schneider & Langer, 1969). In both types the open rhabdom consists of six peripheral rhabdomeres (R_1–R_6) around the central ones (R_7 and/or R_8). The axes of the microvilli are horizontal in R_1, R_2, R_4, R_5 and vertical in R_3 and R_6. In the ventral-type ommatidia the central rhabdom is formed by the two parallel rhabdomeres R_8 with vertical microvilli. The ratio between the cross-section of rhabdomeres with horizontal and vertical microvilli orientation is 1:4 (Schneider & Langer, 1969). The field of view of the ventral eye region extends laterally and medially up to 60° and −15° from the vertical, respectively (Bohn & Täuber, 1971). Hamman & Langer (1980) found visual pigments with sensitivity maxima at 350 nm (UV), 460 nm (blue) and 525 nm (green) in the dark-adapted equatorial eye region of *Gerris lacustris*. These results agree well with that of the recent study of Bartsch (1991), who was able to distinguish an orthogonal system with vertical and horizontal alignments of the polarization sensitivity. The green and blue receptors have a high polarization sensitivity. In the blue receptors, the direction of maximum sensitivity is always horizontal, whereas in the green receptors it is horizontal or vertical.

Schneider & Langer (1969) suggested that the ventral rhabdom specialization in the *Gerris* eye has a screening function against surface-reflected light to gain a better view into the water. In their opinion the light reflected from the water surface is always horizontally polarized, so it is filtered by the rhabdomeres with vertical microvilli. This vertical direction, on the other hand, is optimal for perceiving light from water, which is partially vertically polarized because of refraction at the water surface. However, the ventral eye region (30° or more ventrally) receives only a very small amount of surface-reflected light (only a few percent of the incoming intensity; see Fig. 7), i.e. there may not be much reason for filtering it. On the other hand, under a clear sky with the sun near the horizon, the surface-reflected skylight is mainly vertically polarized at right angles to the solar meridian (Fig. 6B–D). Then the ventral eye region perceives efficiently rather than filters the surface-reflected light. The Schneider–Langer hypothesis is thus not fully supported by the RPPs presented in this paper.

The reflectivity of the flat water surface is relatively small within an angle of view of 60° from the vertical, independently of the meteorological conditions (Fig. 7). Outside this angle, so much light is reflected that waterstriders may be unable to see through the water surface. The reflection glare from this region cannot be filtered by the equatorial-type ommatidia. Furthermore, because of the refraction of light at the water surface, the underwater field of view of waterstriders is so distorted for angles of view larger than 60° from the vertical that detection of motion of

underwater prey or predator is virtually almost impossible (Varjú & Horváth, 1989; Horváth & Varjú, 1990). Similar to backswimmers (Horváth & Varjú, 1995), waterstriders thus have a transparent window on the water surface, through which they can look into the water, but outside that window they can detect only the bright water surface. The coincidence of this transparent window with the net field of view of the two ventral eye regions ($2 \times 60^\circ$) in waterstriders is remarkable. This fact supports the hypothesis that one of the functions of the specialized ventral eye region is to look into the water. Nevertheless, waterstriders can see the underwater world only poorly, because of the low spatial resolution of the ventral part of their eyes, where the interommatidial angles are 5–10° (Dahmen, 1991). The high polarization sensitivity of the visual cells in the waterstrider's ventral ommatidia (Bartsch, 1991) may have the function of enhancing the contrast between underwater enemies and their background. Fish, for instance, have highly reflective scales which can efficiently reflect visible light and also a small amount of UV light (Land, 1972).

A further function of the polarization sensitivity of the waterstrider's ventral eye region is the detection of water (Schwind, 1991), which happens in the green range of the spectrum (Rudolf Schwind, personal communication). Water detection could be mediated by the peripheral subsystem R_1–R_6 with orthogonal microvilli-alignments. On the basis of the work of Bartsch (1991), this subsystem might be a two-channel green-sensitive polarization analyser.

4.3. THE VENTRAL POLARIZATION-SENSITIVE AREA IN THE BACKSWIMMER *NOTONECTA GLAUCA*

In the apposition compound eye of the water bug backswimmer (*Notonecta glauca*), the rhabdom is open. The six peripheral rhabdomeres R_1–R_6 are grouped around the two central fused rhabdomeres R_7 and R_8. In the median eye region, with optical axes pointing from 60° ventral to 80° dorsal, the microvilli of the central rhabdomeres are horizontal. In the ventral eye region, where the optical axes of the ommatidia point 70° or more ventrally, the microvilli of rhabdomeres R_7 and R_8 are horizontally and vertically aligned and have a high polarization sensitivity in the UV range of the spectrum (ventral PSA) (Schwind, 1983*a*). Here, rhabdomeres R_1–R_6 contain a pigment with a sensitivity maximum at 560 nm (yellowish-green), while rhabdomeres R_7–R_8 contain an UV-sensitive (345 nm) visual pigment (Schwind *et al*., 1984). These UV receptors are thought to be significant in the localization of water during the flight (Schwind *et al*., 1984).

The angle of the longitudinal axis of *Notonecta* is 15° to the horizontal during forward flight, making the field of view of its ventral PSA forward from the vertical over a maximum of 35°. Therefore, from a remote distance, water is detected by the eye region directly beneath the dorsal part, where microvilli R_7 and R_8 are horizontal. The spectral characteristics of this eye region have not been studied, but in all probability rhabdomeres R_7 and R_8 here are UV- and/or violet-sensitive (Schwind *et al*., 1984). Water viewed by subsystem R_7–R_8 with a grazing angle to the surface is a prominent optical cue for detection by intensity contrast (Schwind, 1983*b*, 1985*a*). Nevertheless, the UV-sensitive PSA with orthogonal microvilli is a better system for water detection. If the only function of the PSA of backswimmer was the detection and identification of water, it would be more efficient if this PSA were extended over the entire ventral eye region and not only over 70° or more ventrally from the longitudinal body axis. In this case, water could already be detected from a remote distance by the PSA.

Once the flying *Notonecta* has approached the water, the polarized UV light reflected from the surface is detected and analysed by its ventral PSA, and elicits the descent and the plunge reaction if the degree of polarization is greater than a certain value (Schwind, 1983*b*, 1984*a*). This plunge reaction can be elicited only in the presence of horizontally polarized UV light with E-vector perpendicular to the median sagittal plane of the animal (Schwind, 1984*b*). Unpolarized UV light elicits only the positive phototactic behaviour (Schwind, 1985*b*). The slight raising of the body axis before the plunge, observed by Schwind (1983*b*, 1984*a*), could serve to perceive the Brewster zone. With the body in the normal flight position, the ventral PSA of the eye looks perpendicular at the water surface, where the degree of polarization of reflected light is relatively small (Fig. 3). But when the body axis is slightly raised before the plunge, it is aligned at about 36° to the horizon. Then, the ventral PSA looks in the direction of the strongly horizontally polarized Brewster zone, whose direction is 37° (Brewster angle) from the water surface (Figs 3 and 6). This gradient of the surface-reflected polarization perceived by the ventral PSA might contribute to the plunge (Schwind, 1984*a*).

Water surfaces with a small degree of polarization and mainly vertical polarization are not attractive to backswimmers (Schwind, 1985*a*). Under clear skies and for lower elevations of the sun from the horizon, the regions of the flat water surface at right angles to the solar meridian reflect mainly vertically polarized light (Fig. 6C, D)—in some places with a relatively small degree of polarization (Fig. 3C, D) and

reflectivity (Fig. 7C, D). So, when a flying *Notonecta* approaches the water from a remote distance at right angles to the solar meridian, the ventral eye region directly beneath the dorsal part—with horizontal microvilli R_7 and R_8—may be inappropriate for water detection except for light reflected from the relatively narrow Brewster zone (if visible). In this case, the insect may avoid that part of the water surface, from which vertically polarized light is reflected, rather than being attracted by it, and the probability of successful water detection may be reduced.

4.4. THE POLARIZATION-SENSITIVE VENTRAL EYE REGION IN THE DRAGONFLY *HEMICORDULIA TAU*

In the apposition compound eye of *Hemicordulia tau* there are eight retinula cells. However, only the so-called full-size typical cells contribute to the fused rhabdom. The ventral retina is tiered; the distal ommatidium is delineated by the contribution of cell R_1 to the rhabdom. It has either horizontally or vertically aligned microvilli (with horizontal or vertical polarization-sensitivity) with similar frequency. Cell R_1 is thought to be the polarization-sensitive UV cell in the ventral distal retina (Laughlin, 1976; Laughlin & McGinnes, 1978). In the ventral retina, the retinula cells fall into two distinct spectral sensitivity classes: single pigment and linked pigment cells (Laughlin, 1976). The former have a sensitivity maximum at 360 nm (UV), 440 nm, (blue), or 510 nm (green). The UV and green cells are far more common than the blue cell. The single pigment blue and UV cells of the ventral ommatidia have a high polarization sensitivity, whereas the single pigment green cells are insensitive to polarized light (Laughlin, 1976). In the opinion of Laughlin (1976), the polarization sensitive cells in the ventral retina may form a horizon detector for dragonflies flying over water. The orthogonal subsystem R_1 could be used for maintaining a horizontal orientation of the head maximizing the difference between their outputs. Alternatively, these cells could act as a water detector and help in providing territorial landmarks.

In principle, water detection can be performed in *Hemicordulia tau* either by the ventral distal blue receptors or by the orthogonal subsystem of the ventral distal UV receptors R_1. The role of the blue receptors in this process is doubtful because there are not any other retinula cells with horizontal microvilli as in subsystem R_1. For water detection by phototaxis in the blue range of the spectrum, blue receptors with horizontal microvilli would be needed as a minimum requirement. Thus, cells R_1, forming a crossed system, are the only candidate for water detection.

The hypothesis that the ventral eye region may give a dragonfly, flying over water, access to a natural horizon is not yet behaviourally tested. Horizon detection might also be performed by subsystem R_1. The flat water surface could be an ideal natural horizon for dragonflies flying above it only if the reflected light is exactly horizontally polarized in any direction of view. This is the case when the sky is overcast (Fig. 3F) and the ideal case is well approximated when the sky is clear and the sun is near the zenith (Fig. 6A, B). In any other case, however, the RPP at flat water surfaces has a strong degree and direction of polarization gradients, particularly at right angles to the solar meridian (Figs 3C, D and 6C, D). Regions of the water surface with very small degrees of polarization (Fig 3C, D) and/or with directions of polarization that depart strongly from the horizontal (Fig. 6C, D) are insufficient as optical cues for horizon detection. Under partly cloudy skies (Fig. 4) and/or over undulating water surfaces, further significant departures arise from the above-mentioned ideal case. The only appropriate horizon detector over flat water surfaces is the narrow band of the ventral eye region that scans the Brewster zone (Figs 3, 4 and 6).

This work originated during the time the author was on scholarships in the Institute for Zoology of the University of Regensburg (Germany) and at the Department for Biological Cybernetics of the University of Tübingen (Germany). The financial support of the Bayerisches Staatsministerium für Unterricht, Kultus, Wissenschaft und Kunst (Munich, Germany) and the István Széchenyi Scholarship Foundation (Budapest, Hungary) is gratefully acknowledged. I am grateful to Prof. Dr. Rudolf Schwind, Dr. Klaus Bartsch and Dr. Hans-Jürgen Dahmen, who read and commented on an earlier version of the manuscript. Thanks are due to the anonymous referees for their valuable comments.

REFERENCES

BARTSCH, K. (1991). Die funktionelle und strukturelle Regionalisierung des Auges der Wasserläufer. Ph.D. Dissertation, Tübingen: Eberhard Karls University.

BENDELE, H. (1986). Mechanosensory cues control chasing behaviour of whirligig beetles (Coleoptera, Gyrinidae). *J. comp. Physiol.* **A 158,** 405–411.

BOHN, H. & TÄUBER, U. (1971). Beziehungen zwischen der Wirkung polarisierten Lichtes auf das Elektroretinogramm und der Ultrastruktur des Auges von *Gerris lacustris* L. *Z. vergl. Physiol.* **72,** 32–53.

CHEN, H. S. & RAO, C. R. N. (1968). Polarization of light on reflection by some natural surfaces. *Br. J. appl. Phys.* (*J. Phys. D*) **1,** 1191–1200.

COULSON, K. L. (1988). *Polarization and Intensity of Light in the Atmosphere*. Hampton, VA: A. Deepak Publishing.

DAHMEN, H.-J. (1991). Eye specialisation in waterstriders: an adaptation to life in a flat world. *J. comp. Physiol.* **A 169,** 623–632.

FENT, K. (1986). Polarized skylight orientation in the desert ant *Cataglyphis*. *J. comp. Physiol.* **A 158,** 145–150.

FRISCH, K. VON (1949). Die Polarization des Himmelslichtes als orientierender Faktor bie Tänzen der Biene. *Experientia* **5,** 142–148.
GATES, D. M. (1980). *Biophysical Ecology*. Berlin: Springer-Verlag.
GUENTHER, R. D. (1990). *Modern Optics*, pp. 61–87 Duke University: John Wiley & Sons.
HAMANN, B. & LANGER, H. (1980). Sehfarbstoffe im Auge des Wasserläufers *Gerris lacustris* L. *Verh. Dtsch. Zool. Ges*, 337.
HARDIE, R. C. (1984). Properties of photoreceptors R_7 and R_8 in dorsal marginal ommatidia in the compound eyes of *Musca* and *Calliphora*. *J. comp. Physiol.* **A 154,** 157–167.
HAWRYSHYN, C. W. (1992). Polarization vision in fish. *Am. Sci.* **80(2),** 164–175.
HORRIDGE, G. A., MARCELJA, L., JAHNKE, R. & MATIC, T. (1983). Single electrode studies on the retina of the butterfly *Papilio*. *J. comp. Physiol.* **A 150,** 271–294.
HORVÁTH, G. & VARJÚ, D. (1990). Geometric optical investigation of the underwater visual field of aerial animals. *Math. Biosci.* **102,** 1–19.
HORVÁTH, G. & VARJÚ, D. (1995). Underwater refraction-polarization patterns of skylight perceived by aquatic animals through Snell's window of the flat water surface. *Vision Res.*, in press.
JELLEY, J. V. (1989). Sea waves: their nature, behaviour, and practical importance. *Endeavour* (*New Series*) **13,** 148–156.
JERLOV, N. G. (1976). *Optical Oceanography*. Amsterdam: Elsevier.
KÖNNEN, G. P. (1985). *Polarized Light in Nature*. Cambridge: Cambridge University Press.
LABHART, T. (1980). Specialized photoreceptors at the dorsal rim of the honeybee's compound eye: polarizational and angular sensitivity. *J. comp. Physiol.* **A 141,** 19–30.
LABHART, T. (1986). The eletrophysiology of photoreceptors in different eye regions of the desert ant, *Cataglyphis bicolor*. *J. comp. Physiol.* **A 158,** 1–7.
LABHART, T., HODEL, B. & VALENZUELA, I. (1984). The physiology of the cricket's compound eye with particular reference to the anatomically specialized dorsal rim area. *J. comp. Physiol.* **A 155,** 289–296.
LAND, M. F. (1972). The physics and biology of animal reflectors. In: *Progress in Biophysics and Molecular Biology* (Butler, J. A. V. & Noble, D., eds) pp. 75–106. Oxford: Pergamon Press.
LAUGHLIN, S. B. (1976). The sensitivities of dragonfly photoreceptors and the voltage gain of transduction. *J. comp. Physiol.* **111,** 221–247.
LAUGHLIN, S. & MCGINNESS, S. (1978). The structure of dorsal and ventral regions of a dragonfly retina. *Cell Tissue Res.* **188,** 427–447.
MANDELBROT, B. B. (1983). *The Fractal Geometry of Nature*, pp. 233–243. San Francisco: Freeman.
MURPHEY, R. K. (1971). Motor control of orientation to prey by the waterstrider. *Gerris remigis*. *Z. vergl. Physiol.* **72,** 150–167.
ROSSEL S. (1989). Polarization sensitivity in compound eyes. In: *Facets of Vision* (Stavenga, D. G. & Hardie, R. C., eds) pp. 298–316. Berlin: Springer-Verlag.
SCHNEIDER, L. & LANGER, H. (1969). Die Struktur des Rhabdoms im "Doppelauge" des Wasserläufers *Gerris lacustris*. *Z. Zellforsch.* **99,** 538–559.
SCHWIND, R. (1983*a*). Zonation of the optical environment and zonation in the rhabdom structure within the eye of the backswimmer, *Notonecta glauca*. *Cell Tissue Res.* **232,** 53–63.
SCHWIND, R. (1983*b*). A polarization-sensitive response of the flying water bug *Notonecta glauca* to UV light. *J. comp. Physiol.* **150,** 87–91.
SCHWIND, R. (1984*a*). The plunge reaction of the backswimmer *Notonecta glauca*. *J. comp. Physiol.* **A 155,** 319–321.
SCHWIND, R. (1984*b*). Evidence for true polarization vision based on a two-channel analyzer system in the eye of the water bug *Notonecta glauca*. *J. comp. Physiol.* **A 154,** 53–57.
SCHWIND, R. (1985*a*). Sehen unter und über Wasser, Sehen vom Wasser: Das Sehsystem eines Wasserinsektes. *Naturwissenschaften* **72,** 343–352.
SCHWIND, R. (1985*b*). A further proof of polarization vision of *Notonecta glauca* and a note on threshold intensity for eliciting the plunge reaction. *Experientia* **41,** 466–467.
SCHWIND, R. (1991). Polarization vision in water insects and insects living on a moist substrate. *J. comp. Physiol.* **A 169,** 531–540.
SCHWIND, R. & HORVÁTH, G. (1993). Reflection-polarization pattern at water surfaces and correction of a common representation of the polarization pattern of the sky. *Naturwissenschaften* **80,** 82–83.
SCHWIND, R., SCHLECHT, P. & LANGER, H. (1984). Microspectrophotometric characterization and localization of three visual pigments in the compound eye of *Notonecta glauca* L. (Heteroptera). *J. comp. Physiol.* **A 154,** 341–346.
STOCKHAMMER, K. (1959). Die Orientierung nach der Schwingungsrichtung linear polarisierten Lichtes und ihre sinnesphysiologischen Grundlagen. *Ergebn. Biol.* **21,** 23–56.
VARJÚ, D. & HORVÁTH, G. (1989). Looking into the water with a facet eye. *Biol. Cybernet.* **62,** 157–165.
WATERMAN, T. H. (1981). Polarization sensitivity. In: *Handbook of Sensory Physiology Vol.* VII/6B. *Comparative Physiology and Evolution of Vision in Invertebrates B*: *Invertebrate Visual Centers and Behavior I* (Autrum, H., ed) pp. 281–469. Berlin: Springer-Verlag.
WEHNER, R. (1989). The hymenopteran skylight compass: matched filtering and parallel coding. *J. expl Biol.* **146,** 63–85.
WEHNER, R. & STRASSER, S. (1985). The POL area of the honeybee's eye: behavioral evidence. *Physiol. Entomol.* **10,** 337–349.
WESTPHAL, U. (1984). Die Besiedlung künstlicher Kleingewässer in Abhängigkeit von Fläche und Substrat. *Dissert*, *Univ. Marburg*, Lahn, Görich und Weiershäuser, Marbug.
WIESE, K. (1972). Das mechanorezeptorische Beuteortungssystem von *Notonecta*. I. Die Funktion des tarsalen Scolopidialorgans. *J. comp. Physiol.* **78,** 83–102.
WILCOX, R. S. (1972). Communication by surface waves: mating behavior of a water strider (Gerridae). *J. comp. Physiol.* **80,** 255–266.
ZWICK, P. (1990). Emergence, maturation and upstream oviposition flights of Plecoptera from Breitenbach, with notes on the adult phase as a possible control of stream insect populations. *Hydrobiol.* **194,** 207–223.

APPENDIX A

Degree of Polarization of Skylight

In a Rayleigh atmosphere, the degree of linear polarization of skylight can be expressed by

$$\delta = \delta_{\max} \frac{\sin^2 \gamma}{1 + \cos^2 \gamma}, \qquad \text{(A.1)}$$

where γ is the angular distance between the celestial point observed and the sun (Coulson, 1988). In the Rayleigh model the maximum degree of polarization, $\delta_{\max}$, is 100%. However, the number of atmospherical perturbatory effects (e.g. multiple scattering, ground reflection, the presence of dust and molecular anisotropies) cause deviations from the ideal Rayleigh model. One can partly take into consideration these effects using an empirical relationship between $\delta_{\max}$ and the zenith distance θ_s of the sun. This approximation is called the semi-empirical Rayleigh model. Polarization patterns for $\theta_s = 0^\circ$ (sun at the zenith), 30°, 60° and 90° (sun at the horizon) are determined in this paper when the empirical values of $\delta_{\max}$ are 56%, 63%, 70% and 77%, respectively, for clear atmosphere

(Coulson, 1988). The cosine of angle γ can be expressed by

$$\cos\gamma=\sin\theta_s\sin\theta\cos\varphi+\cos\theta_s\cos\theta, \quad \text{(A.2)}$$

where θ and φ are the angular distances of the point observed from the zenith and from the solar meridian, respectively.

APPENDIX B

Direction of Polarization of Skylight

The direction of polarization means the alignment of the major axis of the polarization ellipse of partially linearly polarized light. The maximum of the electric field vector (that is, the half of the major axis of the polarization ellipse) is called the E-vector. At any point in the semi-empirical Rayleigh atmosphere, the direction of polarization is perpendicular to the plane of the triangle formed by the sun, the observer and the point observed. Thus the E-vector can be characterized by the unity vector

$$e=v\cos\alpha+h\sin\alpha,$$

$$v=(-\cos\theta\cos\varphi,-\cos\theta\sin\varphi,\sin\theta),$$

$$h=(-\sin\varphi,\cos\varphi,0) \quad \text{(B.1)}$$

in the point $(1,\theta,\varphi)$ of the spherical coordinate system representing the firmament, where α is the direction of E-vector measured from the meridian of the point observed. Using spherical geometry, the sine and cosine of angle α can be expressed by

$$\sin\alpha=\frac{\cos\theta_s-\cos\theta(\sin\theta_s\sin\theta\cos\varphi+\cos\theta_s\cos\theta)}{\sin\theta\sqrt{1-(\sin\theta_s\sin\theta\cos\varphi+\cos\theta_s\cos\theta)^2}},$$

$$\cos\alpha=\frac{\sin\theta_s\sin\varphi}{\sin\theta\sqrt{1-(\sin\theta_s\sin\theta\cos\varphi+\cos\theta_s\cos\theta)^2}}. \quad \text{(B.2)}$$

Except the neutral Arago, Babinet and Brewster points, positioned in the vicinity of the solar and anti-solar points of the firmament, the semi-empirical Rayleigh model describes well the celestial polarization patterns as a function of the zenith distance of the sun (Können, 1985; Coulson, 1988), at least for biological purposes (see e.g. Waterman, 1981; Wehner, 1989). It would be very complicated to describe mathematically the above-mentioned neutral points, because their characteristics depend strongly on the meterological conditions. For instance, the position of the Arago point depends on the wavelength of light, the elevation of the sun and the extent of the reflection of light from the Earth's surface (Coulson, 1988).

APPENDIX C

Reflection Polarization of Unpolarized Incident Light

The polarization ellipse of unpolarized light is circular. The degree of linear polarization of reflected light for unpolarized incident light (Guenther, 1990) is

$$\delta_r(\theta_i)=\frac{\rho_h(\theta_i)^2-\rho_v(\theta_i)^2}{\rho_h(\theta_i)^2+\rho_v(\theta_i)^2} \quad \text{(C.1)}$$

where

$$\rho_h(\theta_i)=\frac{n_a\cos\theta_i-\sqrt{n_w^2-n_a^2\sin^2\theta_i}}{n_a\cos\theta_i+\sqrt{n_w^2-n_a^2\sin^2\theta_i}}, \quad \text{(C.2)}$$

and

$$\rho_v(\theta_i)=\frac{n_w^2\cos\theta_i-n_a\sqrt{n_w^2-n_a^2\sin^2\theta_i}}{n_w^2\cos\theta_i+n_a\sqrt{n_w^2-n_a^2\sin^2\theta_i}} \quad \text{(C.3)}$$

are the amplitude reflection coefficients for horizontal and vertical polarization of incident light, respectively; n_a and n_w are the refractive indices of air and water, θ_i is the angle of incidence measured from the vertical (Guenther, 1990). When the incident light is unpolarized, the direction of polarization of reflected light is always horizontal. For the Brewster angle $\theta_i^{(B)}=\text{arc}\tan(n_w/n_a)$ it follows that $\delta_r[\theta_i^{(B)}]=1$ and $\rho_v[\theta_i^{(B)}]=0$. The reflectivity of the water surface for unpolarized incident light (Guenther, 1990) is

$$R(\theta_i)=\frac{\rho_h(\theta_i)^2+\rho_v(\theta_i)^2}{2}. \quad \text{(C.4)}$$

APPENDIX D

Reflection Polarization of Partially Linearly Polarized Incident Skylight

Apart from the above-mentioned neutral Arago, Babinet and Brewster points, the skylight is partially linearly polarized (Coulson, 1988). The polarization ellipse of the electric field vector $\boldsymbol{E}$ of skylight is described by

$$E(\varphi_i,\alpha_i,\epsilon)=\frac{E_{\min}}{\sqrt{1-\epsilon^2\cos^2(\varphi_i-\alpha_i)}},$$

$$E_{\min}=E_{\max}\sqrt{1-\epsilon^2}, \quad \text{(D.1)}$$

where $E_{\min}$ and $E_{\max}$ are half of the minor and major axes, α_i is the direction of major axis (with respect to the plane of incidence), $\epsilon = \sqrt{1-(E_{\min}/E_{\max})^2}$ is the excentricity of the ellipse, and angle φ_i is measured from the plane of incidence. The relationships between the degree of linear polarization δ and the excentricity ϵ of the polarization ellipse are

$$\delta = \frac{\epsilon^2}{2-\epsilon^2}, \quad \epsilon = \sqrt{\frac{2\delta}{1+\delta}}. \tag{D.2}$$

The electric field amplitude of partially linearly polarized reflected skylight can be expressed by

$$E_r(\varphi_i, \theta_i, \alpha_i, \epsilon) = E_{\min}\sqrt{\frac{\rho_h(\theta_i)^2 \sin^2\varphi_i + \rho_v(\theta_i)^2\cos^2\varphi_i}{1-\epsilon^2\cos^2(\varphi_i-\alpha_i)}}. \tag{D.3}$$

The spatial distribution of the electric field vector of reflected skylight described by (D.3) is an oval. One has to determine the extrema $E_r^{(\min)}$ and $E_r^{(\max)}$ of function (D.3) and then the degree of linear polarization and the direction of major axis of the reflection-polarization oval. Since this analytical problem results in a fourth-order equation for extrema $E_r^{(\min)}$ and $E_r^{(\max)}$, the numerical treatment is more expedient. The reflectivity of the water surface for partially linearly polarized incident light is

$$R \equiv \frac{\int_0^{\pi} E_r^2(\varphi_i)\,\mathrm{d}\varphi_i}{\int_0^{\pi} E^2(\varphi_i)\,\mathrm{d}\varphi_i} = \frac{\sqrt{1-\epsilon^2}}{\pi}\int_0^{\pi}\frac{\rho_h^2\sin^2\varphi_i + \rho_v^2\cos^2\varphi_i}{1-\epsilon^2\cos^2(\varphi_i-\alpha_i)}\,\mathrm{d}\varphi_i. \tag{D.4}$$

Since it is very complicated to determine analytically the integral (D.4), numerical integration is necessary.